JACS
JOURNAL OF THE AMERICAN CHEMICAL SOCIETY
Article
pubs.acs.org/JACS

Energetic Multifunctionalized Nitraminopyrazoles and Their Ionic Derivatives: Ternary Hydrogen-Bond Induced High Energy Density Materials

Ping Yin,[†] Damon A. Parrish,[‡] and Jean'ne M. Shreeve*[,†]

[†]Department of Chemistry, University of Idaho, Moscow, Idaho 83844-2343, United States
[‡]Naval Research Laboratory, Code 6030, Washington, D.C. 20375-5001, United States

Supporting Information

ABSTRACT: Diverse functionalization was introduced into the pyrazole framework giving rise to a new family of ternary hydrogen-bond induced high energy density materials. By incorporating extended cationic interactions, nitramine-based ionic derivatives exhibit good energetic performance and enhanced molecular stability. Performance parameters including heats of formation and detonation properties were calculated by using *Gaussian 03* and *EXPLO5* v6.01 programs, respectively. It is noteworthy to find that 5-nitramino-3,4-dinitropyrazole, **4**, has a remarkable measured density of 1.97 g cm^{-3} at 298 K, which is consistent with its crystal density (2.032 g cm^{-3}, 150 K), and ranks highest among azole-based CHNO compounds. Energetic evaluation indicates that, in addition to the molecular compound **4**, some ionic derivatives, **9**, **11**, **12**, **17**, **19**, and **22**, also have high densities (1.83−1.97 g cm^{-3}), excellent detonation pressures and velocities (P, 35.6−41.6 GPa; v_D, 8880−9430 m s^{-1}), as well as acceptable impact and friction sensitivities (IS, 4−30 J; FS, 40−240 N). These attractive features highlight the application potential of nitramino hydrogen-bonded interactions in the design of advanced energetic materials.

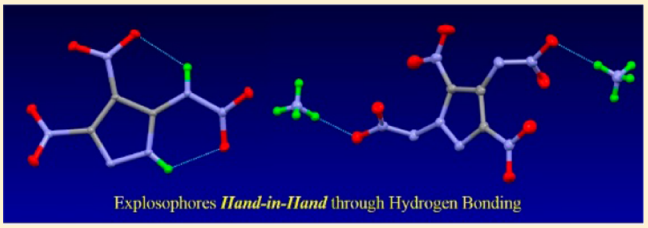

INTRODUCTION

Development of modern energetic materials is significant in material science research. Driven by increasing demands from both military and civilian applications, structural design of energetic molecules has to meet diverse standards, for example, performance properties, environmental compatibility, as well as safety concerns.[1−4] A typical molecule of high energy density materials (HEDMs) is composed of fuel and oxidizer moieties, which can be found in many energetics currently used, such as 2,4,6-trinitrotoluene (TNT),[5] pentaerythritol tetranitrate (PETN),[6] and 1,3,5-trinitrotriazacyclohexane (RDX).[7] In general, incorporation of numerous explosophores (e.g., NO_2, N_3, and ONO_2) tends to improve the density and detonation performance. However, excess compression of functional groups onto a limited backbone leads to decreased sensitivity to mechanical stimulation. Given this background, seeking a balance between high performance and good molecular stability is the main challenge in the design of advanced HEDMs.

As an interesting interaction between hydrogen and other atoms, hydrogen bonding has been found in multiple applications in chemical and physical science.[8,9] By cleverly introducing energetic groups as proton acceptors, strong hydrogen bonds can be formed which serve as a promising tool for construction of HEDMs.[10−12] The enhanced inter- and intramolecular interactions in the molecule give rise to compact packing and thus smaller volume, which are conducive to improving the density and stability of these materials.[13] This design strategy is best exemplified by 1,3,5-triamino-2,4,6-trinitrobenzene (TATB). Compared to 1,3,5-trinitrobenzene with a density of 1.676 g cm^{-3},[3,14] TATB has the remarkably higher density of 1.937 g cm^{-3} originating primarily from the stronger hydrogen bonding interactions by virtue of additional amino-functionalization (Scheme 1).[15−17] The hydrogen bonding type featuring consecutive "NO_2−NH_2−NO_2" blocks has been utilized for designing diversified energetic materials.[18,19] Similarly, *N*-oxide is also a favorable alternative block in building of strong hydrogen bonding moieties, for example, 2,6-diamino-3,5-dinitropyrazine-1-oxide (LLM-105).[20,21] The inherent proton-accepting ability of the N-oxide and nitro groups

Scheme 1. Hydrogen-Bonding Blocks in TATB and LLM-105

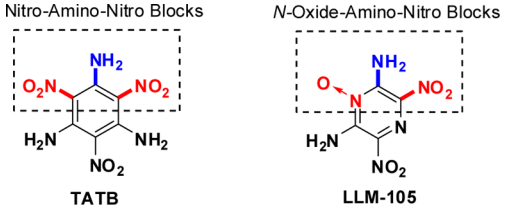

Received: January 21, 2015
Published: March 25, 2015

DOI: 10.1021/jacs.5b00714
J. Am. Chem. Soc. 2015, 137, 4778−4786

Scheme 2. Synthesis of Multifunctionalized Nitraminopyrazoles and Their Ammonium Salts

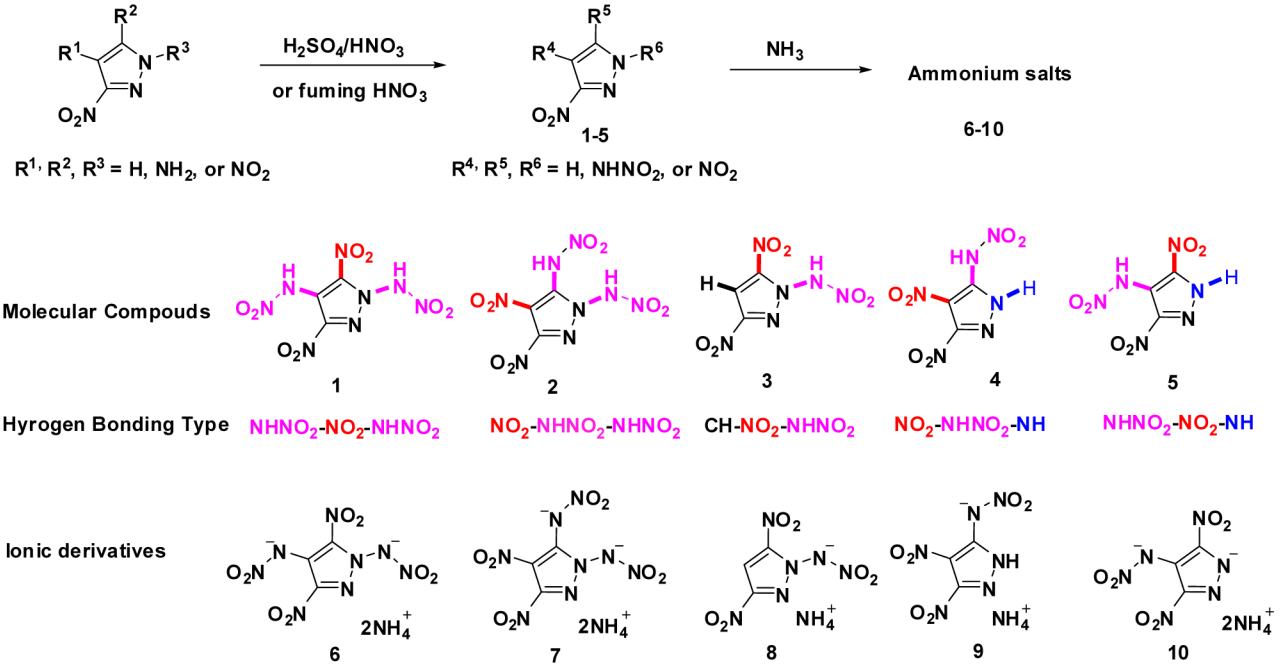

enables strong intramolecular interactions, giving rise to high density and low sensitivity.

Multiple hydrogen-bond interactions between an amino group and nitro and N-oxide groups provide a highly efficient strategy for improving density and stability. However, enhancing detonation performance is still the main challenge, which is mainly caused by the negative oxygen balance and low heat of formation. Recently, the nitramino group has been explored as an energy-rich functionality with nitrogen-rich heterocycles.[22−25] By combining the benefits from high heat of formation and good molecular formula, nitramino-based compounds and their ionic derivatives show favorable overall energetic properties. From the viewpoint of hydrogen bonding formation, the nitramino moiety consists of both hydrogen donator and acceptor, that is, amino and nitro groups respectively, which are capable of forming consecutive interactions toward HEDMs.

Rational design strategy of HEDMs not only requires an intelligent distribution of various energetic functionalities, but also needs to consider their compatibilities with molecular backbones. Five-membered azole and six-membered azine moieties represent the most widely used energetic frameworks, which generally feature high density, positive heat of formation, and good thermal stability. The compatibility between explosophores and backbones has been investigated via the energetic characteristics of fully nitrated heterocycles. While fully nitrated six-membered azines are not the stable form based on experimental and theoretical studies, many fully nitrated five-membered azoles are found widely.[26−30] Representing the latter, 3,4,5-trinitropyrazole (TNP) shows a good balance between energetic performance and molecular stability strikingly highlighting the pyrazole ring as a unique nitro-compatible backbone.[31−33]

In our continuing efforts to pursue new HEDMs, we are highly interested in developing a new effective design strategy to meet the requirements of both higher performance and less sensitivity. The synthesis and characterization of ternary hydrogen-bond induced nitraminopyrazoles and their ionic derivatives are now reported. These multifunctionalized energetic materials feature strong inter- and intramolecular interactions between nitro, amino, and nitramine, that gives rise to high density, excellent performance, and good stability. All compounds are characterized by multinuclear NMR and IR spectroscopy, elemental analyses, and differential scanning calorimetry (DSC). The experimental and calculated data confirm the favorable compromise between energetic properties and molecular stability, which highlight ternary hydrogen-bonding interactions as a promising strategy toward high performance and low sensitive energetic materials.

RESULTS AND DISCUSSION

Synthesis. Various C-amino and N-amino substituted nitropyrazoles are chosen as precursors to develop ternary hydrogen bonding interactions.[34−37] Although N-amination of pyrazoles was studied previously, we now use a convenient and straightforward route for this synthesis that employs hydroxylamine-*O*-sulfonic acid. 1,4-Diamino-3,5-dinitropyrazole, 1,5-diamino 3,4-dinitropyrazole, and 1-amino-3,5-dinitropyrazole were prepared in good yield. Considering the highly reactive nature of the N-amino moiety, nitration of these N-amino compounds was carried out carefully at −10 °C in the presence of sulfuric and fuming nitric acids, giving rise to the corresponding nitramines (**1**−**3**). In contrast, 5-nitramino-3,4-dinitropyrazole (**4**) was readily obtained using fuming nitric acid at 0−5 °C. Similarly, nitration of 4-amino-3,5-dinitropyrazole with mixed acid (70% HNO_3 and concentrated H_2SO_4) resulted in 4-nitramino-3,5-dinitropyrazole (**5**).[38] As a result, five different types of hydrogen bonding were constructed. Compound **4** is a stable neat product at room temperature, whereas the other neutral molecules (**1**−**3**, **5**) are only stable in ether solution. Although **4** was described earlier,[39] different characteristics in the ^{13}C and ^{15}N NMR spectra were found in this work. To obtain further confirmation, **4** was characterized by using single-crystal X-ray diffraction. When the nitramines **1**−**5** were reacted with ammonia in methanol, ionic derivatives

DOI: 10.1021/jacs.5b00714
J. Am. Chem. Soc. 2015, 137, 4778−4786

Table 1. Physical Properties of Nitraminopyrazole (4) and Energetic Salts (6−20, and 22−23)

compd	T_d [°C][a]	d [g cm^{-3}][b]	ΔH_f kJ mol^{-1}/[kJ g^{-1}][c]	P [GPa][d]	v_D [ms^{-1}][e]	IS [J][f]	FS [N][g]	OB [%][h]
4	135	1.97	173.8/0.80	41.6	9430	4	40	14.68
6	139	1.80	143.2/0.46	35.1	8982	12	120	5.13
7	141	1.74	141.9/0.45	32.8	8759	10	120	5.13
8	194	1.77	205.4/0.87	34.1	8748	15	120	3.40
9	195	1.83	144.2/0.61	35.6	8880	30	240	3.40
10[i]	170	1.77	−77.3/−0.31	31.0	8511	35	360	−6.35
11	180	1.86	293.7/1.17	38.7	9176	10	120	0
12	166	1.86	193.7/0.77	38.5	9195	10	80	9.56
13	171	1.72	122.3/0.44	28.3	8319	40	360	−8.66
14	200	1.79	232.3/0.80	32.2	8745	24	160	−10.96
15	177	1.78	488.9/1.62	31.9	8645	20	160	−10.56
16	183	1.81	320.4/1.01	31.5	8629	30	240	−12.62
17	153	1.84	720.5/2.27	37.4	9170	6	60	−5.03
18	142	1.77	416.7/0.79	32.8	8652	20	120	3.04
19	130	1.88	450.0/1.34	39.5	9237	8	80	2.37
20	153	1.75	328.6/1.17	33.8	9040	7	120	−11.35
22	141	1.85	264.2/0.77	40.2	9410	8	80	13.95
23	152	1.75	489.3/1.42	35.7	9066	5	60	0
RDX	204	1.81	80.0/0.36	34.9	8748	7	120	0
HMX	280	1.90	104.8/0.36	39.5	9320	7	120	0

[a]Decomposition temperature (onset). [b]Density measured by gas pycnometer (25 °C). [c]Heat of formation. [d]Detonation pressure (calculated with *EXPLO5* v6.01). [e]Detonation velocity (calculated with *EXPLO5* v6.01). [f]Impact sensitivity. [g]Friction sensitivity. [h]Oxygen balance (based on CO) for $C_aH_bO_cN_d$, $1600(c - a - b/2)/MW$, MW = molecular weight. [i]Reference 38.

(**6**−**10**) were prepared in good yield and high purity (Scheme 2).

To evaluate the different ammonium pyrazolates (**5**−**10**), energetic performance, impact and friction sensitivity, and thermal stability properties were investigated (Table 1). Among them, **9** outperforms all in both detonation properties and molecular stability. Hence, we were interested in designing and synthesizing more valuable 5-nitramino-3,4-dinitropyrazole-based ionic derivatives. Using **4** with equimolar amounts of nitrogen-rich bases, the reactions in aqueous solutions gave rise to energetic salts (**11**−**19**) in nearly quantitative yields (Scheme 3).

It was not possible to form a dication from **4** using excess hydroxylamine or ammonia. In comparison, dihydrazinium 5-nitramino-3,4-dinitropyrazolate (**20**) was prepared successfully by reacting **4** with 2 equiv of hydrazine monohydrate. However, **20** shows lower density and detonation performance than the monocationic analogue **11**. Additionally, dihydroxylammonium salt **22** and dihydrazinium salt **23** were synthesized using the corresponding chloride salts and disilver *N*,*N*′-(3,5-dinitro-1*H*-pyrazol-1,4-diyl)dinitramidate (**21**), which was obtained by metathesis of diammonium *N*,*N*′-(3,5-dinitro-1*H*-pyrazol-1,4-diyl)dinitramidate (**6**) and silver nitrate (Scheme 3).

Scheme 3[a]

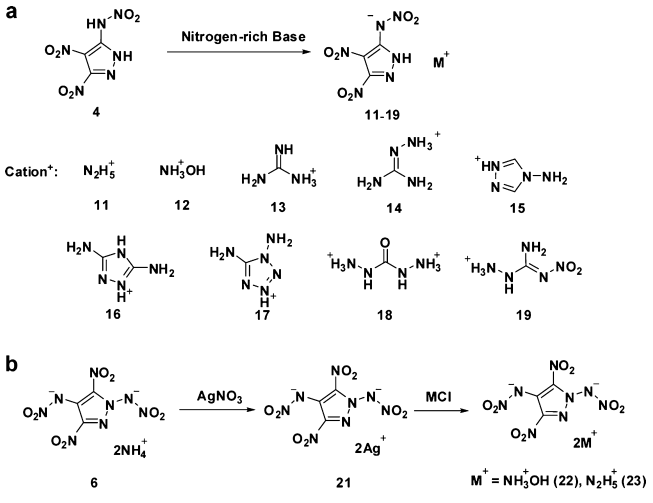

[a](a) Synthesis of monocationic 5-nitramino-3,4-dinitropyrazolates. (b) Synthesis of 1,4-nitramino-3,5-dinitropyrazole-based salts.

Spectroscopy. All new nitraminopyrazoles and their ionic derivatives were characterized by NMR, IR spectroscopy, and elemental analysis. The characteristic infrared absorption bands for the nitro group were observed for all compounds in the 1300−1600 cm^{-1} region. In the ^{13}C NMR spectrum of diammonium 1,4-nitramino-3,5-dinitropyrazolate (**6**), three signals for the anion appear at 142.2, 134.6, 123.6 ppm. Due to the presence of different substituents on the ring, carbon resonances of other anions were observed between 100−150 ppm. ^{15}N NMR spectroscopic data were measured and representative results are given in Figure 1. The signals of all *C*-nitro and *N*-nitro groups can be assigned to resonances ranging from δ = 0 to −30 ppm. The ^{15}N {H} NMR spectrum of **6** shows nine signals at δ = −3.95 (N4), −15.76 (N7), −21.61(N5), −28.40 (N8), −85.28 (N2), −109.40 (N1), −147.68 (N3), −158.21 (N6), and −358.29 (N9) ppm. For **4**, **9**, and **11**, the resonances at ∼−105 and ∼−190 ppm are assigned to N1 and N2 of the pyrazole ring, respectively. In contrast, the pyrazole backbone of **6** appears at −85.28 and −109.40 ppm. Both ammonium cations of **6** and **9** are observed at higher field (δ = −359.30 ppm), whereas the hydrazinium cation of **11** appears slightly lower (δ = −331.32 ppm).

Single Crystal X-ray Structure Analysis. A crystal of **4**, suitable for single-crystal X-ray diffraction, was obtained by dissolving **4** in acetone and letting chloroform diffuse into the solution, whereas **6**, **9**·H_2O, and **11** were crystallized from methanol solution. Compound **4** crystallizes in the triclinic

DOI: 10.1021/jacs.5b00714
J. Am. Chem. Soc. 2015, 137, 4778−4786

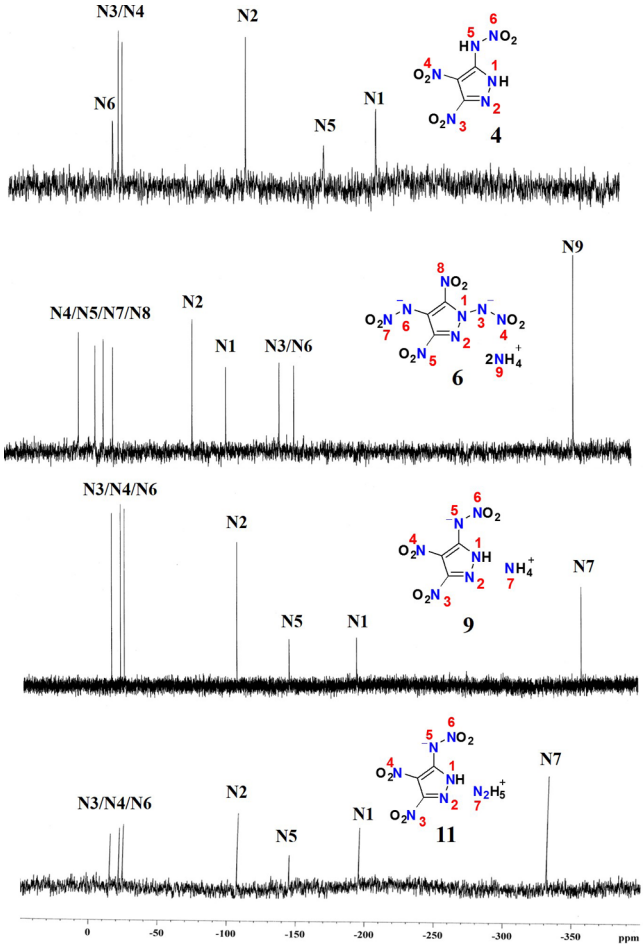

Figure 1. ^{15}N NMR spectra of **4**, **6**, **9**, and **11**.

space group P-1 and with four molecules per unit cell (Figure 2). It has a calculated density of 2.032 g cm^{-3} at 150 K. The 4-

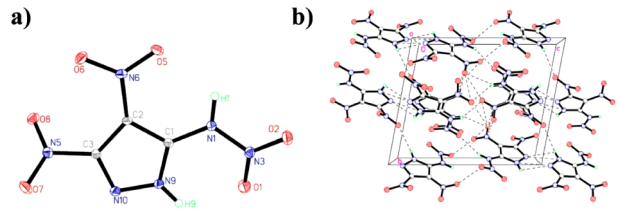

Figure 2. (a) Single-crystal X-ray structure of **4**. (b) Packing diagram of **4** viewed along the *a* axis.

nitro, 5-nitramino groups, and pyrazole ring are nearly planar due to the consecutive hydrogen-bond interactions (N1−C1−C2−N6, 0.3(2)°; N3−N1−C1−C2, 173.34(9)°; O5−N6−C2−C1, 9.9(1)°; H1−N1−N3−O1, 176(1) °). In these pyrazole derivatives, the bond lengths of the two C-nitro groups range between 1.4169(11) and 1.4549(11) Å, which are similar to those found for 3,4,5-trinitropyrazole (1.4418(14)−1.4538(14) Å).

The unit cell of diammonium *N*,*N*′-(3,5-dinitro-1H-pyrazol-1,4-diyl)dinitramidate (**6**) crystallizes with a calculated density (1.832g cm^{-3} at 150 K) in the monoclinic space group $P2_1/c$. As can be seen in the crystal structure given in Figure 3, there are extensive hydrogen bonding interactions between the ammonium cation and the nitroamino groups. The two *C*-NO_2

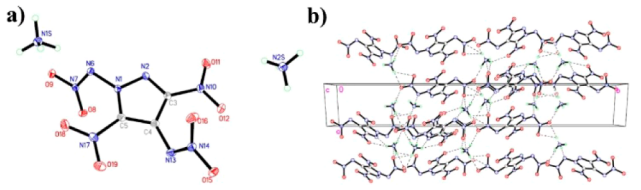

Figure 3. (a) Single-crystal X-ray structure of **6**. (b) Packing diagram of **6** viewed along the *c* axis.

groups and the pyrazole ring are nearly coplanar with a torsion angle of N(1)−C(5)−N(17)−O(19), 171.67(13)°, whereas the two *N*-NO_2 groups are twisted out of the pyrazole ring plane with a torsion angle of C(5)−C(4)−N(13)−N(14), −119.08(16)°.

Ammonium 5-nitramino-3,4-dintropyrazolate monohydrate (**9**·H_2O) crystallizes in the triclinic space group P-1 with two molecules in the unit cell (Figure 4), and has a calculated

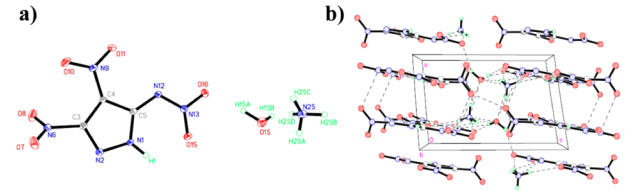

Figure 4. (a) Single-crystal X-ray structure of **9**·H_2O. (b) Packing diagram of **9**·H_2O viewed along the *b* axis.

density of 1.831 g cm^{-3} at 150 K. The geometry of the pyrazole anion is comparable to that observed in its neutral precursor (**4**). In spite of deprotonation, the nitramino group lies in the plane of the pyrazole ring as supported by the N1−C5−N12−N13 torsion angle of −2.7(3)°, C4−C5−N12−N13 torsion angle of 179.13(18)°, and C5−N12−N13−O15 torsion angle of −3.0(3)°. The main change of deprotonated nitramine is observed in bond lengths of C5−N12 (1.365(2) Å) and N12−N13 (1.323(2) Å), which are slightly shorter than that of **4** (1.369(1) Å −1.418(2) Å). Additionally, it is interesting to find that the NH group of pyrazole anion has an intramolecular hydrogen bonding interaction with O11. Hydrazinium 5-nitramino-3,4-dintropyrazolate (**11**) crystallizes with a calculated density (1.886 g cm^{-3} at 150 K) in the monoclinic space group $P2_1/n$ (Figure 5), and the anion crystal structure is similar to that in **9**·H_2O (see the Supporting Information).

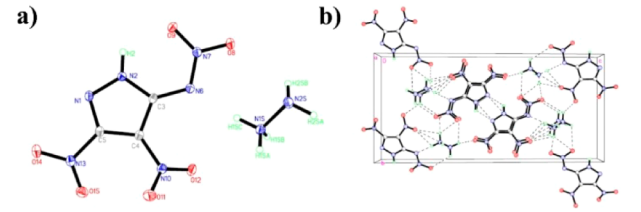

Figure 5. (a) Single-crystal X-ray structure of **11**. (b) Packing diagram of **11** viewed along the *a* axis.

As trinitropyrazole (TNP) has been previously investigated, it is of interest to compare the properties of pyrazole analogues with different energetic functionalities.[40] The interatomic H···O distance between NH and NO_2 group is a significant criteria to evaluate the hydrogen-bonding strength. For TNP, the intramolecular H···O distances between the 5-NO_2 group and

DOI: 10.1021/jacs.5b00714
J. Am. Chem. Soc. 2015, 137, 4778−4786

the pyrazole NH group range from 2.538 to 2.583 Å. In comparison, nitramine **4** shows a remarkably shorter intramolecular H···O distance, which can be confirmed by both the 4-NO_2/5-$NHNO_2$ interactions (2.130−2.187 Å) and the 5-NHO_2/1-NH interactions (2.063−2.083 Å). To examine the unit cell packing, the packing coefficient (PC) was calculated according to the reference method.[41−43] Nitramine **4** shows a higher PC value (0.79) than that of TNP (0.72), indicating a more efficient unit cell packing toward the highly dense characteristics (**4**, 2.032 g cm^{-3} at 150 K; TNP, 1.929 g cm^{-3} at 100 K).

Other than intramolecular interaction, **4** and ionic derivatives (**6**, **9**·H_2O, and **11**) show more diversified intermolecular H-bonding interactions. As the nitro group is a favorable acceptor, the majority of hydrogen bonds belong to N−H···O interactions, whereas a minority of hydrogen bonds belong to N−H···N interactions between the two neighboring pyrazole rings.

Although strong intramolecular interactions are observed in **4**, the intermolecular interactions are weak because all H···O and H···N distance are above 2.3 Å. For **6** and **11**, some stronger intermolecular interactions are found between cations and nitramino groups (H···O, 2.015−2.084 Å). In comparison, the relatively weaker H-bonding interactions of **9**·H_2O are observed between 4-NO_2 and 1-NH groups (H···O, 2.195 Å). However, this interaction style of **9**·H_2O is conducive to form a layered crystal structure and good unit cell packing, which are supported by the distance between pyrazole centroids (3.519 Å) and packing coefficient (0.77).

Physicochemical Properties. The phase-transition and thermal stabilities of all compounds were determined by DSC. With the exception of **4** and **15** that melt at 129 and 165 °C, respectively, all other compounds (**6**−**14**, **16**−**20**, and **22**−**23**) decompose without melting. While neutral compound **4** decomposes at 135 °C, its salts (**9**−**20**) are more thermally stable (142−200 °C), with the exception of **19** (130 °C).

The experimental densities of these compounds are in the range of 1.72−1.97 g cm^{-3}, which are comparable to the currently used energetic materials, such as RDX (1.80 g cm^{-3}) and cyclo-1,3,5,7-tetramethylenene-2,4,6,8-tetranitramine (HMX, 1.91 g cm^{-3}). It is noteworthy that **4** has an impressive calculated crystal density of 2.032 g cm^{-3} at 150 K, which is the highest value to date for the crystal density of an azole-based CHNO energetic material. Compared to some reported azole derivatives, for example, 3-nitro-5-nitramino-1*H*-1,2,4-triazole (1.938 g cm^{-3} at 100 K) and 5-nitrimino-1*H*-tetrazole (1.867 g cm^{-3} at 100 K),[44,45] the remarkably higher density of **4** may be attributed to the consecutive nitro-nitramino-amino intramolecular interactions of ternary hydrogen bonds. As an exceptional precursor, neutralization of **4** with nitrogen rich bases gives rise to a series of high-density energetic salts. Among them, salts **11**, **12**, **19**, and **22** show excellent densities of 1.86, 1.86, 1.88, and 1.85 g cm^{-3}, respectively. In contrast to the dihydrazinium salt, **20**, with lower density (1.75 g cm^{-3}), the higher density of the monohydrazinium salt **11** arises from the NH group of the pyrazole ring, which forms strong hydrogen bond interactions with the neighboring nitro group and the hydrazinium cation.

In order to evaluate the energetic properties, computation of the heats of formation were performed by using the *Gaussian03* (revision D.01) suite of programs.[46] Based on the method of isodesmic reactions (see the Supporting Information), the gas phase enthalpy of formation was computed and the enthalpy of reaction was obtained by combining the MP2/6-311++G** energy difference for the reactions, the scaled zero point energies (ZPE), values of thermal correction (HT), and other thermal factors. According to these data, the gas phase enthalpy of these species can be extracted.

The enthalpy of sublimation was calculated by using Trouton's rule. Solid-state heats of formation of the neutral compound **4** were calculated with eq 1 (T_m is the melting temperature).[47,48]

$$\Delta H_f = \Delta H_f\,(g) - \Delta H_{sub} = \Delta H_f\,(g) - 188\ [J\ mol^{-1}\ K^{-1}] \times T_m \quad (1)$$

Scheme 4. Born−Haber Cycle for the Formation of Energetic Pyrazolates Where *a*, *b*, *c*, and *d* Are the Number of Moles of the Respective Products

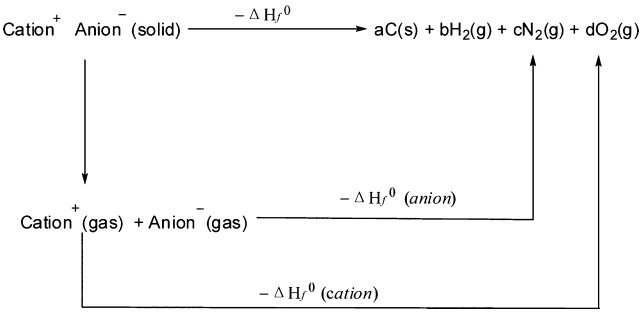

Based on the Born−Haber energy cycle (Scheme 4), the solid phase heat of formation of ionic compounds can be simplified by eq 2.

$$\Delta H_f^\circ\,(\text{salt, 298 K}) = \Delta H_f^\circ\,(\text{cation, 298 K}) + \Delta H_f^\circ\,(\text{anion, 298 K}) - \Delta H_L \quad (2)$$

In eq 2, the lattice energy (ΔH_L) of energetic salts could be predicted by using the formula suggested by the literature [eq 3]:[49]

$$\Delta H_L = U_{POT} + [p(n_M/2 - 2) + q(n_X/2 - 2)]RT \quad (3)$$

in which n_M and n_X depend on the nature of the ions M^{p+} and X^{q-}, respectively, and are equal to three for monatomic ions, five for linear polyatomic ions, and six for nonlinear polyatomic ions. The equation for lattice potential energy U_{POT} has the form [eq 4]:

$$U_{POT}\ [kJ\ mol^{-1}] = \gamma(\rho/M)_{1/3} + \delta \quad (4)$$

in which ρ (g cm^{-3}) is the density, M is the chemical formula mass of the ionic compound, and values for the coefficients γ (kJ mol cm^{-1}) and δ (kJ mol^{-1}) are taken from the literature.[49]

As seen in Table 1, 5-nitramino-3,4-dintropyrazole (**4**) has a heat of formation of 173.8 kJ mol^{-1} (0.80 kJ g^{-1}), which is slightly greater than that of 3,4,5-trinitropyraozle (147 kJ mol^{-1}, 0.72 kJ g^{1}). Among the ammonium pyrazolates (**6**−**10**), **8** exhibits the highest heat of formation at 205.4 kJ mol^{-1} (0.87 kJ g^{-1}). The heat of formation values for 5-nitramino-3,4-dintropyrazole-based energetic salts (**9**, **11**-**20**) and 1,4-dinitramino-3,5-dintropyrazole-based energetic salts (**22**-**23**)

DOI: 10.1021/jacs.5b00714
J. Am. Chem. Soc. 2015, 137, 4778−4786

range from 122.3 kJ mol^{-1} (0.44 kJ g^{-1}) to 720.5 kJ mol^{-1} (2.27 kJ g^{-1}).

In addition to the heat of formation, detonation properties and impact and friction sensitivities play a major role for new energetic materials. With experimental densities and calculated values for heats of formation in hand, the detonation pressures (P) and velocities (v_D) were calculated by using *EXPLO5* v6.01. The calculated detonation pressures and velocities lie in the ranges from 28.3 to 41.6 GPa, and from 8319 to 9430 m s^{-1}, respectively. Compound **4** exhibits the highest detonation properties (P, 41.6 GPa; v_D, 9430 m s^{-1}), which are significantly superior to the high explosive HMX (P, 39.5 GPa; v_D, 9320 m s^{-1}). Some ionic derivatives of **4** are also exhibit good performance, such as **11** (P, 38.7 GPa; v_D, 9176 m s^{-1}), **12** (P, 38.5 GPa; v_D, 9195 m s^{-1}), **17** (P, 37.4 GPa; v_D, 9170 m s^{-1}), **19** (P, 39.5 GPa; v_D, 9237 m s^{-1}), and **22** (P, 40.2 GPa; v_D, 9410 m s^{-1}).

Impact and friction sensitivity measurements were made using a standard BAM Fallhammer and a BAM friction tester. Not surprisingly the neutral nitramine, **4**, shows relatively sensitive characteristics, with impact sensitivity (IS) of 4 J and friction sensitivity (FS) of 40 N. By pairing with nitrogen-rich cations, its energetic salts are well stabilized with additional ionic and hydrogen bonding, and thus exhibit lower impact and friction sensitivities (IS, 6−40 J; FS, 60−360 N). Among them, the ammonium salt, **9**, has good detonation properties (P, 35.6 GPa; v_D, 8880 m s^{-1}) with low sensitivities (IS, 30 J; IS, 240 N), which are superior to that of RDX (P, 34.9 GPa; v_D, 8749 m s^{-1}; IS, 7 J; IS, 120 N). Oxygen balance (OB) is another important index to evaluate the deficiency or excess of oxygen in a molecule required to convert all carbon into carbon monoxide and all hydrogen into water. Arising from the multiple nitro and nitramino functionalities, **4**−**9**, **12**, **18**, **19**, and **22** have positive oxygen balances, whereas the OB values of **11** and **23** are zero. Other pyrazolates exhibit negative OB values ranging from −12.62% to −5.03%. Compounds **4** and **22** have excellent OB values of 14.68% and 13.95%, respectively, which suggest their application potential as energetic oxidizers.

CONCLUSION

A family of new multifunctionalized nitraminopyrazoles and their nitrogen-rich salts was developed as energetic materials. On the basis of a ternary hydrogen-bonding strategy, considerable effort was focused on designing diversified functionalities by virtue of nitro, nitroamino, and amino groups. All neutral compounds (**1**−**5**) can be stabilized by formation of the corresponding ammonium salts (**6**−**10**). Among these compounds, energetic properties indicate that ammonium 5-nitroamino-3,4-dinitropyrazolate (**9**) competes well with other ammonium pyrazolates (**6**−**8**, **10**) in detonation performance and molecular stability. As promising precursors, **4** and **6**, in reaction with a variety of nitro-rich bases, resulted in salts **11**−**20** and **22**, **23**. These energetic compounds were fully characterized by IR, and NMR spectroscopy, as well as elemental analysis. For compounds **4**, **6**, **9**, and **11**, structure was confirmed with single-crystal X-ray diffraction analyses. With an outstanding density (2.032 g cm^{-3} at 150 K, 1.97 g cm^{-3} at 298 K), **4** exhibits excellent detonation properties (P, 41.6 GPa; v_D, 9430 m s^{-1}) which are superior to those of HMX (P, 39.5 GPa; v_D, 9320 m s^{-1}). In spite of relative high sensitivity characteristics of molecular compound **4** (IS, 4J; FS, 40N), ionic derivatives show enhanced stabilities and excellent properties, which are exemplified by **9** (d, 1.83 g cm^{-3}; P, 35.6 GPa; v_D, 8880 m s^{-1}; IS, 30 J; FS, 240 N), **11** (d, 1.86 g cm^{-3}; P, 38.7 GPa; v_D, 9176 m s^{-1}; IS, 10 J; FS, 120 N), and **22** (d, 1.85 g cm^{-3}, P, 40.3 GPa; v_D, 9410 m s^{-1}; IS, 8 J; FS, 80 N). This work highlights nitroamino-based hydrogen bonding interactions as a favorable strategy for the exploration of new HEDMs.

EXPERIMENTAL SECTION

Safety Precautions. Although we have not encountered any difficulties in preparing these new energetic materials, manipulations must be carried out by using standard safety precautions. All compounds should be handled with extreme care and eye protection and gloves must be worn.

General Methods. All reagents were purchased from Alfa Aesar and AK Scientific in analytical grade and were used as received. ^{1}H and ^{13}C NMR spectra were recorded on a Bruker 300 MHz nuclear magnetic resonance spectrometer operating at 300 and 75 MHz, respectively. ^{15}N NMR spectra were recorded on a Bruker 500 MHz nuclear magnetic resonance spectrometer operating at 50.7 MHz. Chemical shifts for ^{1}H and ^{13}C NMR spectra are reported relative to $(CH_3)_4Si$ and for ^{15}N NMR to CH_3NO_2. D_6-DMSO was used as a locking solvent unless otherwise stated. Elemental analyses (C, H, N) were performed on a CE-440 Elemental Analyzer. Melting and decomposition (onset) points were recorded on a differential scanning calorimeter (TA Instruments Q10) at a scan rate of 5 °C min^{-1}. Impact and friction sensitivity measurements were made using a standard BAM Fallhammer and a BAM friction tester. IR spectra were recorded using KBr pellets with a Biorad model 3000 FTS spectrometer. Densities were determined at room temperature by employing a Micromeritics AccuPyc 1330 gas pycnometer.

X-ray Crystallography. A colorless plate crystal of dimensions 0.12 × 0.10 × 0.02 mm^3 for **4**, a yellow rod of dimensions 0.07 × 0.03 × 0.02 mm^3 for **6**, a yellow plate crystal of dimensions 0.50 × 0.38 × 0.04 mm^3 for **9**·H_2O, and a yellow needle of dimensions 0.14 × 0.01 × 0.01 mm^3 for **11** were mounted on a MiteGen MicroMesh using a small amount of Cargille immersion oil. Data were collected on a Bruker three-circle platform diffractometer equipped with a SMART APEX II CCD detector. The crystals were irradiated using graphite monochromated Mo Kα radiation (λ = 0.71073). An Oxford Cobra low temperature device was used to keep the crystals at a constant 150(2) K during data collection.

Data collection was performed, and the unit cell was initially refined using *APEX2* [v2010.3-0].[50] Data reduction was performed using *SAINT* [v7.68A][51] and *XPREP* [v2008/2].[52] Corrections were applied for Lorentz, polarization, and absorption effects using *SADABS* [v2008/1].[53] The structure was solved and refined with the aid of the programs in the *SHELXTL-plus* [v2008/4] system of programs.[54] The full-matrix least-squares refinement on F^2 included atomic coordinates and anisotropic thermal parameters for all non-H atoms. The H atoms were included using a riding model. CCDC 1024259 (**4**), 1040463 (**6**), 1024260 (**9**·H_2O), and 1040462 (**11**) contain the supplementary crystallographic data for this paper. These data can be obtained free of charge from The Cambridge Crystallographic Data Centre via www.ccdc.cam.ac.uk/data_request/cif.

General Procedure for N-Amino Nitropyrazoles. *N*-Amino nitropyrazoles were prepared according to the modified literature method.[34−37] Nitropyrazole (10 mmol) was added to a solution of sodium hydroxide (2.00 g, 50 mmol) and sodium dihydrogen phosphate monohydrate (4.83 g, 35 mmol) in distilled water (50 mL). The mixture was heated to 80 °C, and hydroxylamine-*O*-sulfonic acid (40 mmol, 4.52 g) was added portion-wise within 1 h; the pH was adjusted to 6.5−7.5 by addition of sodium carbonate. The reaction was held at 80 °C for 6 h. After cooling to room temperature, the desired product was isolated by filtration or extraction.

1,4-Diamino-3,5-dinitropyrazole.[36] The final mixture was adjusted to pH 8 by addition of sodium carbonate, and the product was collected by filtration. Orange solid (1.15 g, 61% yield). ^{1}H NMR (D_6-DMSO): δ 7.24 (s, 2H), 7.93 (s, 2H). ^{13}C NMR (D_6-DMSO): 134.1, 130.2, 128.0.

DOI: 10.1021/jacs.5b00714
J. Am. Chem. Soc. 2015, 137, 4778−4786

1,5-Diamino-3,4-dinitropyrazole.[37] The final mixture was extracted with ethyl acetate (3 × 15 mL), and then the combined organic phases were dried over Na_2SO_4. The solvent was removed under reduced pressure and the residue was purified by chromatography with hexane/ethyl acetate. Yellowish solid (1.32 g, 70%). ^{1}H NMR (D_6-DMSO): δ 7.63 (s, 2H), 6.36 (s, 2H). ^{13}C NMR (D_6-DMSO): 146.2, 144.4, 107.0.

1-Amino-3,4-dinitropyrazole.[37] The final mixture was extracted with ethyl acetate (3 × 15 mL), and then the combined organic phases were dried over Na_2SO_4. The solvent was removed under reduced pressure, and the residue was purified by chromatography with hexane/ethyl acetate. White solid (1.01 g, 58%). ^{1}H NMR (D_6-DMSO): δ 7.99 (s, 1H), 7.87 (s, 2H). ^{13}C NMR (D_6-DMSO): 147.2, 141.7, 101.2.

*N-(3,4-Dinitro-1H-pyrazol-5-yl)nitramide (**4**).* To ice-cold fuming nitric acid (15 mL) was added 3,4-dinitro-1*H*-pyrazol-5-amine (865 mg, 5 mmol) in small portions, and the reaction was held at 0−5 °C for an additional 15 min. Nitric acid was removed by blowing air, and the residue was dried in vacuo to yield **4**. Yellowish solid (1.03 g, 94% yield). ^{1}H NMR (D_6-DMSO): δ 8.67 (s, 2H). ^{13}C NMR (D_6-DMSO): δ 144.5, 140.0, 124.8. ^{15}N NMR (D_6-DMSO): δ −18.09, −21.94, −24.38, −105.10, −156.31, −190.36. IR (KBr pellet): υ 3375. 3314, 3234, 1621, 1587, 1567, 1514, 1467, 1441, 1333, 1243, 1147, 1057, 984, 866, 842, 743 cm^{-1}. Elemental analysis (%) calcd for $C_3H_2N_6O_6$ (218.08): C, 16.52; H, 0.92; N, 38.54. Found: C, 16.48; H, 0.88; N, 37.54.

*General Procedure for Ammonium Salts **6**−**8**.* *N*-Amino nitropyrazole (2 mmol) was dissolved in concentrated sulfuric acid (10 mL) and cooled to −15 °C in an ice-salt bath. Fuming nitric acid (2 mL) was added dropwise to the cold solution and the reaction mixture was held at ∼−10 °C for 0.5 h. The final solution was poured onto crushed ice (50 g) and extracted with ethyl ether (2 × 10 mL). The combined organic phase was washed with water (5 mL), brine (5 mL), and dried over Na_2SO_4. The ether solution of *N*-nitramino nitropyrazole was treated with 2 mL of ammonia solution (7 N in methanol). After removing all the solvent, the remaining residue was crystallized from methanol to yield the product (**6**−**8**).

*Diammonium N,N′-(3,5-Dinitro-1H-pyrazol-1,4-diyl)-dinitramidate (**6**).* Yellowish solid (399 mg, 64% yield). ^{1}H NMR (D_6-DMSO): δ 7.15 (br, 8H). ^{13}C NMR (D_6-DMSO): δ 142.2, 134.6, 123.6. ^{15}N NMR (D_6-DMSO): δ −3.95, −15.76, −21.61, −28.40, −85.28, −109.40, −147.68, −158.21, −358.29. IR (KBr pellet): υ 3294, 3173, 3053, 1577, 1508, 1419, 1389, 1321, 1115, 1018, 837 cm^{-1}. Elemental analysis (%) calcd for $C_3H_8N_{10}O_8$ (312.16): C, 11.54; H, 2.58; N, 44.87. Found: C, 12.05; H, 2.61; N, 43.71.

*Diammonium N,N′-(3,4-Dinitro-1H-pyrazol-1,5-diyl)-dinitramidate hydrate (**7**).* Yellow solid (322 mg, 52% yield). ^{1}H NMR (D_6-DMSO): δ 7.18 (br, 8H). ^{13}C NMR (D_6-DMSO): δ 143.5, 143.3, 115.6. IR (KBr pellet): υ 3258, 3055, 1643, 1542, 1503, 1380, 1277, 1094, 1040, 1003, 860, 810 cm^{-1}. Elemental analysis (%) calcd for $C_3H_8N_{10}O_8{\cdot}H_2O$ (330.17): C, 10.91; H, 3.05; N, 42.42. Found: C, 10.69; H, 2.77; N, 42.75.

*Ammonium N-(3,5-Dinitro-1H-pyrazol-1-yl)nitramidate (**8**).* Yellowish solid (421 mg, 76% yield). ^{1}H NMR (D_6-DMSO): δ 8.01 (s, 1H), 7.07 (br, 8H). ^{13}C NMR (D_6-DMSO): δ 148.7, 142.9, 101.4. ^{15}N NMR (D_6-DMSO): δ −4.71, −23.69, −30.38, −74.87, −108.73, −147.89, −358.28. IR (KBr pellet): υ 3429, 3146, 1563, 1508, 1456, 1402, 1379, 1334, 1306, 1138, 1087, 887, 832, 737 cm^{-1}. Elemental analysis (%) calcd for $C_3H_5N_7O_6$ (235.12): C, 15.33; H, 2.14; N, 41.70. Found: C, 15.51; H, 1.97; N, 41.73.

*Ammonium N-(3,4-Dinitro-1H-pyrazol-5-yl)nitramidate (**9**).* A solution of **4** (436 mg, 2 mmol) in 5 mL of methanol was stirred at room temperature while excess ammonia (7 N in methanol, 1 mL) was added. After removing all the solvent, the remaining residue was crystallized from methanol to yield **9**. Yellowish solid (421 mg, 76% yield). ^{1}H NMR (D_6-DMSO): δ 13.53 (br, 1H), 7.09 (s, 4H). ^{13}C NMR (D_6-DMSO): δ 149.0, 146.2, 112.4. ^{15}N NMR (D_6-DMSO): δ −14.43, −20.88, −23.66, −106.27, −144.50, −193.88, −358.30. IR (KBr pellet): υ 3573, 3422, 3254, 1630, 1557, 1505, 1413, 1297, 1209, 1065, 984, 839, 806,761 cm^{-1}. Elemental analysis (%) calcd for $C_3H_5N_7O_6$ (235.12): C, 15.33; H, 2.14; N, 41.70. Found: C, 15.40; H, 2.12; N, 41.02.

*Hydrazinium N-(3,4-Dinitro-1H-pyrazol-5-yl)nitramidate (**11**).* A solution of **4** (436 mg, 2 mmol) in 5 mL of distilled water was stirred at room temperature while hydrazine monohydrate (0.1 mL, 2 mmol) was added. After removing all the solvent, the remaining residue was dried under vacuum to yield **11**. Yellowish solid (487 mg, 97% yield). ^{1}H NMR (D_6-DMSO): δ 8.03 (br, 5H). ^{13}C NMR (D_6-DMSO): δ 148.8, 146.2, 112.3. ^{15}N NMR (D_6-DMSO): δ −14.46, −20.99, −23.77, −106.79, −144.57, −195.12, −331.32. IR (KBr pellet): υ 3358, 3286, 3071, 2878, 2646, 1553, 1503, 1418, 1368, 1309, 1227, 1151, 1092, 1067, 966, 843, 801 cm^{-1}. Elemental analysis (%) calcd for $C_3H_6N_8O_6$ (250.13): C, 14.41; H, 2.42; N, 44.80. Found: C, 14.32; H, 2.36; N, 44.44.

*Hydroxylammonium N-(3,4-Dinitro-1H-pyrazol-5-yl)nitramidate (**12**).* A solution of **4** (436 mg, 2 mmol) in 5 mL of distilled water was stirred at room temperature while hydroxylamine monohydrate (0.1 mL, 2 mmol) was added. After removing all the solvent, the remaining residue was dried in vacuo to yield **12**. Yellow solid (482 mg, 96% yield). ^{1}H NMR (D_6-DMSO): δ 10.59 (br, 4H). ^{13}C NMR (D_6-DMSO): δ 148.9, 146.2, 112.3. ^{15}N NMR (D_6-DMSO): δ −14.68, −20.65, −23.33, −104.55, −144.18, −188.80, −293.58. IR (KBr pellet): υ 3340, 3206, 2959, 2778, 1559, 1509, 1405, 1360, 1290, 1231, 1165, 1069, 993, 849, 808, 763 cm^{-1}. Elemental analysis (%) calcd for $C_3H_5N_7O_7$ (251.11): C, 14.35; H, 2.01; N, 39.04. Found: C, 14.07; H, 2.02; N, 38.69.

*Guanidinium N-(3,4-Dinitro-1H-pyrazol-5-yl)nitramidate (**13**).* A solution of **4** (436 mg, 2 mmol) in 5 mL of distilled water was stirred at room temperature while guanidinium carbonate (360 mg, 2 mmol) was added. After removing all the solvent, the remaining residue was dried under vacuum to yield **13**. Yellow solid (514 mg, 93% yield). ^{1}H NMR (D_6-DMSO): δ 6.88 (s, 6H). ^{13}C NMR (D_6-DMSO): δ 158.0, 148.8, 146.1, 112.3. ^{15}N NMR (D_6-DMSO): δ −14.33, −20.81, −23.61, −106.65, −144.23, −194.61, −305.18 (t, J = 91.3 Hz). IR (KBr pellet): υ 3429, 3206. 1665, 1549, 1499, 1452, 1412, 1354, 1300, 1217, 1068, 984, 839, 808, 758 cm^{-1}. Elemental analysis (%) calcd for $C_4H_7N_9O_6$ (277.16): C, 17.33; H, 2.55; N, 45.48. Found: C, 17.27; H, 2.50; N, 45.03.

*Aminoguanidinium N-(3,4-Dinitro-1H-pyrazol-5-yl)nitramidate (**14**).* A solution of **4** (436 mg, 2 mmol) in 5 mL of distilled water was stirred at room temperature while aminoguanidinium bicarbonate (272 mg, 2 mmol) was added. After removing all the solvent, the remaining residue was dried under vacuum to yield **14**. Yellow solid (559 mg, 96% yield). ^{1}H NMR (D_6-DMSO): δ 8.68 (s, 1H), 7.24 (br, 2H), 6.90 (br, 2H), 4.66 (s, 2H). ^{13}C NMR (D_6-DMSO): δ 158.9, 148.8, 146.2, 112.3. IR (KBr pellet): υ 3422, 3347, 3261, 1669, 1553, 1505, 1410, 1306, 1219, 1066, 986, 933, 841, 808, 761, 629 cm^{-1}. Elemental analysis (%) calcd for $C_4H_8N_{10}O_6$ (292.17): C, 16.44; H, 2.76; N, 47.94. Found: C, 16.40; H, 2.72; N, 47.49.

*4-Amino-triazolium N-(3,4-Dinitro-1H-pyrazol-5-yl)nitramidate (**15**).* A solution of **4** (436 mg, 2 mmol) in 5 mL of distilled water was stirred at room temperature while 4*H*-1,2,4-triazol-4-amine (168 mg, 2 mmol) was added. After removing all the solvent, the remaining residue was dried in vacuo to yield product **15**. Yellow solid (568 mg, 94% yield). ^{1}H NMR (D_6-DMSO): δ 9.43 (s, 5H). ^{13}C NMR (D_6-DMSO): δ 148.8, 146.1, 144.1, 112.3. IR (KBr pellet): υ 3349, 3298, 3116, 2992, 2889, 1634, 1553, 1507, 1419, 1294, 1215, 1137, 1063, 980, 936, 841, 808, 758, 675 cm^{-1}. Elemental analysis (%) calcd for $C_5H_6N_{10}O_6$ (302.16): 19.87; H, 2.00; N, 46.35. Found: C, 19.91; H, 1.99; N, 46.00.

*3,5-Diamino-triazolium N-(3,4-Dinitro-1H-pyrazol-5-yl)-nitramidate (**16**).* A solution of **4** (436 mg, 2 mmol) in 5 mL of distilled water was stirred at room temperature while 3,5-diaminotriazole (198 mg, 2 mmol) was added. After removing all the solvent, the remaining residue was dried under vacuum to yield **16**. Yellow solid (601 mg, 95% yield). ^{1}H NMR (D_6-DMSO): δ 8.07 (br, 6H). ^{13}C NMR (D_6-DMSO): δ 152.3, 148.8, 146.2, 112.3. IR (KBr pellet): υ 3409, 3345, 3208, 1693, 1663, 1549, 1502, 1412, 1297, 1218, 1056, 841, 808, 761, 738 cm^{-1}. Elemental analysis (%) calcd for

DOI: 10.1021/jacs.5b00714
J. Am. Chem. Soc. 2015, 137, 4778−4786

$C_3H_7N_{11}O_6$ (317.18): C, 18.93; H, 2.22; N, 48.58. Found: C, 18.98; H, 2.25; N, 48.42.

*1,5-Diamino-tetrazolium N-(3,4-Dinitro-1H-pyrazol-5-yl)-nitramidate (**17**).* A solution of **4** (436 mg, 2 mmol) in 5 mL of distilled water was stirred at room temperature while 1,5-diaminotetrazole (200 mg, 2 mmol) was added. After removing all the solvent, the remaining residue was dried under vacuum to yield **17**. Yellowish solid (609 mg, 96% yield). ^{1}H NMR (D_6-DMSO): δ 8.79 (br, 5H). ^{13}C NMR (D_6-DMSO): δ 152.8, 148.8 145.2, 113.0. IR (KBr pellet): υ 3434, 3337, 3294, 1720, 1626, 1555, 1509, 1438, 1355, 1294, 1203, 1066, 983, 841, 808 cm^{-1}. Elemental analysis (%) calcd for $C_4H_6N_{12}O_6$ (318.17): C, 15.10; H, 1.90; N, 52.83. Found: C, 15.02; H, 1.84; N, 52.56.

*Carbohydrazinium Bis[N-(3,4-dinitro-1H-pyrazol-5-yl)-nitramidate] (**18**).* A solution of **4** (436 mg, 2 mmol) in 5 mL of distilled water was stirred at room temperature while carbohydrazide (90 mg, 1 mmol) was added. After removing all the solvent, the remaining residue was dried in vacuo to yield **18**. Yellowish solid (488 mg, 93% yield). ^{1}H NMR (D_6-DMSO): δ 9.83 (s, 2H), 6.68 (br, 6H). ^{13}C NMR (D_6-DMSO): δ 157.7, 148.8, 145.7, 112.3. IR (KBr pellet): υ 3557, 3430, 3316, 3212, 1732, 1622, 1550, 1506, 1410, 1296, 1229, 1067, 984, 843, 808, 761 cm^{-1}. Elemental analysis (%) calcd for $C_7H_{10}N_{16}O_{13}$ (526.25): C, 15.98; H, 1.92; N, 42.59. Found: C, 16.17; H, 1.98; N, 41.41.

*3-Amino-1-nitroguanidinium N-(3,4-Dinitro-1H-pyrazol-5-yl)-nitramidate (**19**).* A solution of **4** (436 mg, 2 mmol) in 5 mL of distilled water was stirred at room temperature while 3-amino-1-nitroguanidine (238 mg, 2 mmol) was added. After removing all the solvent, the remaining residue was dried under vacuum to yield **19**. Yellow solid (625 mg, 93% yield). ^{1}H NMR (D_6-DMSO): δ 9.63 (br, 5H), 8.41 (s, 1H). ^{13}C NMR (D_6-DMSO): δ 158.9, 148.9, 145.4, 113.0. IR (KBr pellet): υ 3379, 3310, 3107, 1645, 1619, 1586, 1503, 1458, 1358, 1297, 1215, 1170, 1067, 1017, 839 cm^{-1}. Elemental analysis (%) calcd for $C_4H_7N_{11}O_8$ (337.17): C, 14.25; H, 2.09; N, 45.70. Found: C, 13.84; H, 2.25; N, 45.82.

*Dihydrazinium N-(3,4-Dinitro-1H-pyrazol-5-yl)nitramidate (**20**).* A solution of **4** (436 mg, 2 mmol) in 5 mL of ethanol was stirred at room temperature while hydrazine monohydrate (0.2 mL, 4 mmol) was added. The precipitate was filtered and dried in vacuo to yield **20**. Yellow solid (476 mg, 84% yield). ^{1}H NMR (D_6-DMSO): δ 5.96 (br, 10H). ^{13}C NMR (D_6-DMSO): δ 149.3, 149.2, 115.0. IR (KBr pellet): υ 3596, 3335, 1620, 1586, 1484, 1452, 1367, 1290, 1159, 1126, 1098, 974, 873, 842, 810, 773, 738 cm^{-1}. Elemental analysis (%) calcd for $C_3H_{10}N_{10}O_6$ (282.17): C, 12.77; H, 3.57; N, 49.64. Found: C, 12.93; H, 3.32; N, 48.20.

*Disilver N,N′-(3,5-Dinitro-1H-pyrazol-1,4-diyl)dinitramidate Hydrate (**21**).* A solution of **6** (614 mg, 2 mmol) in 10 mL of distilled water was stirred at room temperature while silver nitrate (680 mg, 4 mmol) was added. The precipitate was filtered and dried in vacuum to yield **21** (917 mg, 93%). IR (KBr pellet): υ 3589, 1592, 1530, 1450, 1387, 1369, 1326, 1297, 1251, 1125, 1016, 943, 893, 844, 760 cm^{-1}. Elemental analysis (%) calcd for $C_3Ag_2N_8O_8{\cdot}H_2O$ (509.83): C, 7.07; H, 0.40; N, 21.98. Found: C, 7.06; H, 0.36; N, 20.59.

*Dihydroxylammonium N,N′-(3,5-Dinitro-1H-pyrazol-1,4-diyl)-dinitramidate (**22**).* Disilver *N,N′*-(3,5-dinitro-1*H*-pyrazol-1,4-diyl)-dinitramidate hydrate (510 mg, 1 mmol) was added to distilled water (10 mL) and hydroxylammonium chloride (139 mg, 2 mmol). After stirring overnight at ambient temperature, silver chloride was removed by filtration and washed with a small amount of water. The filtrate was concentrated under reduced pressure and dried in vacuo to yield **22** (313 mg, 91%). ^{1}H NMR (D_6-DMSO): δ 10.09 (br, 8H). ^{13}C NMR (D_6-DMSO): δ 149.8, 134.3, 124.0. IR (KBr pellet): υ 3426, 3101, 2950, 2712, 1548, 1509, 1439, 1376, 1332, 1305, 1264, 1188, 1007, 877, 839, 768 cm^{-1}. Elemental analysis (%) calcd for $C_3H_8N_{10}O_{10}$ (344.16): C, 10.47; H, 2.34; N, 40.70. Found: C, 10.39; H, 2.46; N, 38.92.

*Dihydrazinium N,N′-(3,5-Dinitro-1H-pyrazol-1,4-diyl)-dinitramidate (**23**).* Disilver *N,N′*-(3,5-dinitro-1*H*-pyrazol-1,4-diyl)-dinitramidate hydrate (510 mg, 1 mmol) was added to distilled water (10 mL) and hydrazinium chloride (137 mg, 2 mmol). After stirring overnight at ambient temperature, silver chloride was removed by filtration and washed with a small amount of water. The filtrate was concentrated under reduced pressure and dried in vacuo to yield **23** (321 mg, 94%). ^{1}H NMR (D_6-DMSO): δ 7.08 (br, 10H). ^{13}C NMR (D_6-DMSO): δ 141.9, 134.4, 123.7. ^{15}N NMR (D_6-DMSO): δ −3.75, −15.66, −21.23, −28.12, −85.40, −108.91, −148.13, −157.68, −331.57. IR (KBr pellet): υ 3342, 3325, 3266, 3179, 2924, 2805, 2719, 1574, 1535, 1500, 1435, 1371, 1326, 1273, 1201, 1096, 1025, 999, 922, 839, 769 cm^{-1}. Elemental analysis (%) calcd for $C_3H_{10}N_{12}O_8$ (342.19): C, 10.53; H, 2.95; N, 49.12. Found: C, 10.45; H, 2.97; N, 48.68.

■ ASSOCIATED CONTENT

Supporting Information

X-ray crystallographic data for **4**, **6**, **9**·H_2O, and **11**; atomic coordinates, anisotropic displacement parameters, bond lengths, angles, dihedral angles, hydrogen-bonding data, and isodesmic reactions. This material is available free of charge via the Internet at http://pubs.acs.org.

■ AUTHOR INFORMATION

Corresponding Author

*jshreeve@uidaho.edu

Notes

The authors declare no competing financial interest.

■ ACKNOWLEDGMENTS

The authors are grateful for the support of ONR (N00014-12-1-0536) and the Defense Threat Reduction Agency (HDTRA 1-11-1-0034). The authors acknowledge Dr. Orion Berryman (NSF CHE-1337908) for considerable assistance with crystal structures.

■ REFERENCES

(1) Gao, H.; Shreeve, J. M. *Chem. Rev.* **2011**, *111*, 7377−7436.
(2) Fischer, D.; Klapötke, T. M.; Stierstorfer, J. *Angew. Chem., Int. Ed.* **2014**, *53*, 8172−8175.
(3) Dippold, A. A.; Klapötke, T. M. *J. Am. Chem. Soc.* **2013**, *135*, 9931−9938.
(4) Thottempudi, V.; Shreeve, J. M. *J. Am. Chem. Soc.* **2011**, *133*, 19982−19992.
(5) Boddu, V. M.; Viswanath, D. S.; Ghosh, T. K.; Damavarapu, R. *J. Hazard. Mater.* **2010**, *181*, 1−8.
(6) Steinhauser, G.; Giester, G.; Leopold, N.; Wagner, C.; Villa, M.; Musilek, A. *Helv. Chim. Acta* **2010**, *93*, 183−202.
(7) Agrawal, J. P.; Hodgson, R. D. *Organic Chemistry of Explosives*; Wiley: New York, 2007.
(8) Grabowski, S. J. *Chem. Rev.* **2011**, *111*, 2597−2625.
(9) Zhanpeisov, N. U.; Anpo, M. *J. Am. Chem. Soc.* **2004**, *126*, 9439−9444.
(10) Latypov, N. V.; Bergman, J.; Langlet, A.; Wellmar, U.; Bemm, U. *Tetrahedron* **1998**, *54*, 11525−11536.
(11) Mehilal, A. K. S.; Sinha, R. K.; Gandhe, B. R. *J. Hazard. Mater.* **2003**, *102*, 137−145.
(12) Joo, Y.-H.; Shreeve, J. M. *J. Am. Chem. Soc.* **2010**, *132*, 15081−15090.
(13) Ye, C.; Shreeve, J. M. *J. Phys. Chem. A* **2007**, *111*, 1456−1461.
(14) Choi, C. S.; Abel, J. E. *Acta Crystallogr.* **1972**, *B28*, 193−201.
(15) Cady, H. H.; Larson, A. C. *Acta Crystallogr.* **1965**, *18*, 485−496.
(16) Tarver, C. M. *J. Phys. Chem. A* **2010**, *114*, 2727−2736.
(17) Hoffman, D. M.; Fontes, A. T. *Propellants, Explos., Pyrotech.* **2010**, *35*, 15−23.
(18) De Bie, D. A.; Geurtsen, B.; Van der Plas, H. C. *J. Org. Chem.* **1985**, *50*, 484−2487.
(19) Schmidt, R. D.; Lee, G. S.; Pagoria, P. F.; Mitchell, A. R.; Gilardi, R. *J. Heterocycl. Chem.* **2001**, *38*, 1227−1230.

DOI: 10.1021/jacs.5b00714
J. Am. Chem. Soc. 2015, 137, 4778−4786

(20) Averkiev, B. B.; Antipin, M. Y.; Yudin, I. L.; Sheremetev, A. B. *J. Mol. Struct.* **2002**, *606*, 139−146.
(21) Gilardi, R. D.; Butcher, R. J. *Acta Crystallogr.* **2001**, *E57*, o657−o658.
(22) Wang, R.; Xu, H.; Guo, Y.; Sa, R.; Shreeve, J. M. *J. Am. Chem. Soc.* **2010**, *132*, 11904−11905.
(23) Klapötke, T. M.; Petermayer, C.; Piercey, D. G.; Stierstorfer, J. *J. Am. Chem. Soc.* **2012**, *134*, 20827−20836.
(24) Joo, Y-. H.; Shreeve, J. M. *Angew. Chem., Int. Ed.* **2010**, *49*, 7320−7323.
(25) Joo, Y-. H.; Shreeve, J. M. *Angew. Chem., Int. Ed.* **2009**, *48*, 564−567.
(26) Wei, T.; Zhu, W.; Zhang, X.; Li, Y.; Xiao, H. *J. Phys. Chem. A* **2009**, *113*, 9404−9412.
(27) Coburn, M. D.; Hiskey, M. A.; Lee, K. Y.; Ott, D. G.; Stinecipher, M. M. *J. Heterocycl. Chem.* **1993**, *30*, 1593−1595.
(28) Hinshaw, J. C.; Edwards, W. W.; George, C.; Gilardi, R. *J. Heterocycl. Chem.* **1992**, *29*, 1721−1724.
(29) Bagal, L. I.; Pevzner, M. S.; Frolov, A. N.; Sheludyakova, N. I. *Khim. Geterotsikl. Soedin.* **1970**, *6*, 259−264.
(30) Koldobskii, G. I.; Soldatenko, D. S.; Gerasimova, E. S.; Khokhryakova, N. R.; Shcherbinin, M. B.; Lebedev, V. P.; Ostrovskii, V. A. *Russ. J. Org. Chem.* **1997**, *33*, 1771−1783.
(31) Hervé, G.; Roussel, C.; Graindorge, H. *Angew. Chem., Int. Ed.* **2010**, *49*, 3177−3181.
(32) Yin, P.; Zhang, J.; Parrish, D. A.; Shreeve, J. M. *Chem.—Eur. J.* **2014**, *20*, 16529−16536.
(33) Zhang, Y.; Guo, Y.; Joo, Y. H.; Parrish, D. A.; Shreeve, J. M. *Chem.—Eur. J.* **2010**, *16*, 10778−10784.
(34) Dalinger, I. L.; Vatsadze, I. A.; Shkineva, T. K.; Popova, G. P.; Shevelev, S. A. *Synthesis* **2012**, *44*, 2058−2064.
(35) Dalinger, I. L.; Cherkasova, T. I.; Popova, G. P.; Shkineva, T. K.; Vatsadze, I. A.; Shevelev, S. A.; Kanishchev, M. I. *Russ. Chem. Bull. Int. Ed.* **2009**, *58*, 410−413.
(36) He, C.; Zhang, J.; Parrish, D. A.; Shreeve, J. M. *J. Mater. Chem. A* **2013**, *1*, 2863−2868.
(37) Yin, P.; Zhang, J.; He, C.; Parrish, D. A.; Shreeve, J. M. *J. Mater. Chem. A* **2014**, *2*, 3200−3208.
(38) Zhang, Y. Q.; Parrish, D. A.; Shreeve, J. M. *Chem.—Eur. J.* **2012**, *18*, 987−994.
(39) Dalinger, I. L.; Vatsadze, I. A.; Shkineva, T. K.; Popova, G. P.; Ugrak, B. I.; Shevelev, S. A. *Russ. Chem. Bull.* **2010**, *59*, 1631−1638.
(40) Nelyubina, Y. V.; Dalinger, I. L.; Lyssenko, K. A. *Angew. Chem., Int. Ed.* **2011**, *50*, 2892−2894.
(41) Dolomanov, O. V.; Bourhis, L. J.; Gildea, R. J.; Howard, J. A. K.; Puschmann, H. *J. Appl. Crystallogr.* **2009**, *42*, 339−341.
(42) Zhang, C.; Xue, X.; Cao, Y.; Zhou, J.; Zhang, A.; Li, H.; Zhou, Y.; Xu, R.; Gao, T. *CrystEngComm* **2014**, *16*, 5905−5916.
(43) Zhang, J.; Zhang, Q.; Vo, T. T.; Parrish, D. A.; Shreeve, J. M. *J. Am. Chem. Soc.* **2015**, *137*, 1697−1704.
(44) Dippold, A. A.; Klapötke, T. M.; Martin, F. A.; Wiedbrauk, S. *Eur. J. Inorg. Chem.* **2012**, *14*, 2429−2443.
(45) Klapötke, T. M.; Stierstorfer, J. *Helv. Chim. Acta* **2007**, *90*, 2132−2150.
(46) Frisch, M. J.; Trucks, G. W.; Schlegel, H. B.; Scuseria, G. E.; Robb, M. A.; Cheeseman, J. R.; Montgomery, J. A., Jr.; Vreven, T.; Kudin, K. N.; Burant, J. C.; Millam, J. M.; Iyengar, S. S.; Tomasi, J.; Barone, V.; Mennucci, B.; Cossi, M.; Scalmani, G.; Rega, N.; Petersson, G. A.; Nakatsuji, H.; Hada, M.; Ehara, M.; Toyota, K.; Fukuda, R.; Hasegawa, J.; Ishida, M.; Nakajima, T.; Honda, Y.; Kitao, O.; Nakai, H.; Klene, M.; Li, X.; Knox, J. E.; Hratchian, H. P.; Cross, J. B.; Bakken, V.; Adamo, C.; Jaramillo, J.; Gomperts, R.; Stratmann, R. E.; Yazyev, O.; Austin, A. J.; Cammi, R.; Pomelli, C.; Ochterski, J. W.; Ayala, P. Y.; Morokuma, K.; Voth, G. A.; Salvador, P.; Rabuck, J. J.; Raghavachari, K.; Foresman, J. B.; Ortiz, J. V.; Cui, Q.; Baboul, A G.; Clifford, S.; Cioslowski, J.; Stefanov, B. B.; Liu, A. L. G.; Piskorz, P.; Komaromi, I.; Martin, R. L.; Fox, D. J.; Keith, T.; Al-Laham, M. A.; Peng, C.; Nanayakkara, A.; Challacombe, M.; Gill, P. M. W.; Johnson, B.; Chen, W.; Wong, M.; Gonzalez, C.; Pople, J. A. *Gaussian 03*, revision D.01; Gaussian, Inc.: Wallingford CT, 2004.
(47) Westwell, M. S.; Searle, M. S.; Wales, D. J.; Williams, D. H. *J. Am. Chem. Soc.* **1995**, *117*, 5013−5015.
(48) Dippold, A. A.; Klapötke, T. M.; Winter, N. *Eur. J. Inorg. Chem.* **2012**, 3474−3484.
(49) Jenkins, H. D. B.; Tudela, D.; Glasser, L. *Inorg. Chem.* **2002**, *41*, 2364−2367.
(50) *APEX2*, v2010.3-0; Bruker AXS Inc.: Madison, WI, 2010.
(51) *SAINT*, v7.68A; Bruker AXS Inc.: Madison, WI, 2009.
(52) *XPREP*, v2008/2; Bruker AXS Inc.: Madison, WI, 2008.
(53) *SADABS*, v2008/1; Bruker AXS Inc.: Madison, WI, 2008.
(54) *SHELXTL*, v2008/4; Bruker AXS Inc.: Madison, WI, 2008.

DOI: 10.1021/jacs.5b00714
J. Am. Chem. Soc. 2015, 137, 4778−4786